Available online at www.sciencedirect.com
SCIENCE DIRECT®
Journal of Power Sources 115 (2003) 12–18
JOURNAL OF POWER SOURCES
www.elsevier.com/locate/jpowsour

Performance of $La_{0.8}Sr_{0.2}CoO_3$ coated NiO as cathodes for molten carbonate fuel cells

Prabhu Ganesan, Hector Colon, Bala Haran, Branko N. Popov*

Department of Chemical Engineering, Center for Electrochemical Engineering, University of South Carolina, Columbia, SC 29208, USA

Received 6 November 2002; accepted 17 November 2002

Abstract

$La_{0.8}Sr_{0.2}CoO_3$ was coated on NiO (LSC–NiO) cathodes using a sol–gel method. Dissolution studies in molten Li_2CO_3 and K_2CO_3 (62:38 mol%) at 650 °C showed lower Ni dissolution than that of the conventional nickel oxide cathode. Impedance analysis showed that the behavior of the developed cathode is similar to that of nickel oxide. The LSC coated Ni cathode has an over potential of 109 mV at an applied current density of 160 mA/cm^2. The LSC–NiO shows promise as an alternate cathode in molten carbonate fuel cells (MCFCs).

Keywords: Dissolution; MCFC; $La_{0.8}Sr_{0.2}CoO_3$; Nickel oxide

1. Introduction

The molten carbonate fuel cell (MCFC) is a promising power generating system due to its high-energy conversion efficiency accompanied by its low harmful gas emission. However, solubility of nickel oxide cathode in the electrolyte is one of the important problems facing the commercialization of MCFC technology. Nickel oxide reacts with the dissolved CO_2 in the electrolyte according to an acidic dissolution mechanism and dissolves in the molten carbonate during operation. The cation diffuses to the anode side of the electrolyte and is then reduced in the hydrogen atmosphere to metallic nickel. Precipitates of metallic nickel have been found in the electrolyte tile much closer to the anode and this precipitate acts as a sink for further deposition of nickel particles. This growth of the nickel layer eventually leads to a short circuit between the anode and cathode. The dissolution is accelerated under higher CO_2 partial pressure resulting in a decrease of the operating life of the cell. The dissolution of NiO also results in a decrease of the active surface area available for the oxygen reduction reaction resulting in degradation in the cell performance.

More basic molten carbonate melts such as Li/Na carbonate eutectic do not favor the NiO dissolution process and have been used to decrease the Ni dissolution rate in the melt [1,2]. The other approach to counter the nickel dissolution problem is to either modify NiO or to identify alternate cathode materials, which have longer life in the melt. Porous electrodes with good electronic conductivity, chemical stability and proper microstructure therefore offer the excellent choice for MCFC cathodes. Several ceramic materials with small solubility in the melt have been studied as alternatives to NiO. $LiFeO_2$, $LiCoO_2$ [3] and $La_{0.2}Sr_{0.8}CoO_3$ [4] offered initial promise as replacement material for NiO cathodes. $LiCoO_2$ coated nickel cathodes are reported in literature [5,6]. Cobalt was coated mechanically onto nickel powder and used as the cathode [7]. In our earlier study cobalt was coated on to sintered nickel electrode by an electro less plating process and used as a cathode [8]. $LiNi_{0.8}Co_{0.2}O_2$, lithium battery cathode material has also been tried as an alternate for MCFC cathodes [9].

In this work, $La_{0.8}Sr_{0.2}CoO_3$ was coated onto the sintered nickel electrodes and its electrochemical performance has been studied in laboratory scale 3 cm^2 half-cells.

2. Experimental

2.1. Tape casting

Porous nickel cathode was made by a tape casting and sintering process. Nickel (Aldrich) particles were ground

* Corresponding author. Tel.: +1-803-777-7314; fax: +1-803-777-8265.
E-mail address: popov@engr.sc.edu (B.N. Popov).

0378-7753/02/$ – see front matter
PII: S0378-7753(02)00621-3

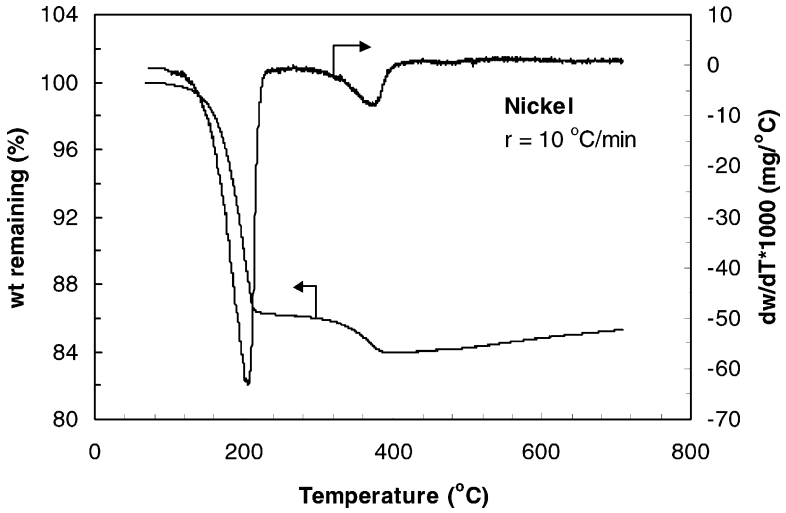

Fig. 1. Thermo gravimetric analysis (TGA) of Ni tape obtained by aqueous tape casting process.

and sieved to obtain uniform particles of size 3–5 μm. The tape casting slurry was prepared by ball milling nickel powder in water with suitable binder (PVA) and plasticizer (glycerol). The ball milling was done in two steps. At the first step, 50 g of nickel powder were added to 5 g of PVA (PVA liquid 15 wt.%) and 1 g of defoamer (Airdefoam™ 60, Air Products). The ingredients were mixed thoroughly with 15 g of water and the slurry was ball milled for 3 h in order to break the weak agglomerates. Next, 9 g of glycerol was added to the above suspension and the resulting slurry was ball milled for an additional 3 h. The slurry was then slightly warmed (50 °C) and degassed using a ROTOVAP® evaporator. The slurry was cooled and then cast using a doctor blade assembly over a glass plate coated with silicone oil. The drying was performed slowly at room temperature for about 48 h. The cast plate nickel tape is then stripped off gently from the glass plate and stored.

2.2. Sintering

Sintering of the tape cast electrodes influences the cathode pore structure and thereby affects its electrochemical performance. TGA was done to determine the optimum heat treatment schedule for sintering. A typical TGA curve for green nickel tape is shown in Fig. 1. The as cast Ni tape is pre-heated at 120 °C for 12 h in order to remove all the crystalline water in the tape. TGA analysis was done by heating the sample from 100 to 650 °C at a rate of 10 °C/min. A steep reduction in weight (15 wt.%) is seen on heating the sample to 200 °C due to the removal of the binder. A secondary weight loss (5 wt.%) is noticed between 300 and 400 °C due to the removal of plasticizer. The removal of all volatile and decomposable organic matter is completed below 400 °C. On heating the sample above 400 °C oxidation of nickel surface takes place. The total weight loss varies between 15 and 20 wt.% depending upon the binder and plasticizer contents in the green tapes. Since, Ni is oxidized beyond 400 °C, it is critical to heat the sample in a reducing atmosphere to prevent oxidation during sintering. Further, the rate of heating should be very slow initially to ensure complete burn out of binder and plasticizer.

Green tapes were cut out to specific area (10 cm × 10 cm) and were placed between two porous alumina plates inside a programmable tube furnace. The heating schedule consists of the following stages: (i) first, start from room temperature and heat to 130 °C at a rate of 1 °C/min in nitrogen atmosphere, (ii) hold the temperature at 130 °C for 10 h, (iii) next, raise the temperature to 230 °C at a rate of 1 °C/min in nitrogen atmosphere, (iv) hold the temperature at 230 °C for 2 h, (v) raise the temperature to 400 °C at 1 °C/min in nitrogen atmosphere, (vi) hold the temperature at 400 °C for 2 h, (vii) finally, raise the temperature to 800 °C at 1 °C/min in hydrogen atmosphere, (viii) hold the temperature at 800 °C for 1 h and (ix) cool to room temperature at 1 °C/min in hydrogen atmosphere.

2.3. $La_{0.8}Sr_{0.2}CoO_3$ coating

$La_{0.8}Sr_{0.2}CoO_3$ precursor gel was prepared as follows. Initially stoichiometric amounts of lanthanum acetate (5.488 g), strontium acetate (0.8588 g) and cobalt acetate (4.9814 g) were dissolved in DI water with constant stirring. Then, citric acid (8.4056 g), a complexing agent dissolved in DI water was added followed by the addition of ethylene glycol (2.4828 g). The pH of the solution was maintained between 8 and 9. The solution was heated for 10 h at 80 °C using a hot plate with constant stirring until it turned into a viscous gel. Nickel electrodes of desired size were cut and dipped in the gel and dried in air for 1 h and then dried in vacuum for 5 h at 90 °C. The dipping was repeated several times to have a uniform coating. The flow chart for the coating is given in Fig. 2. After drying, the electrodes were heat treated at different temperatures varying from 300 to 900 °C.

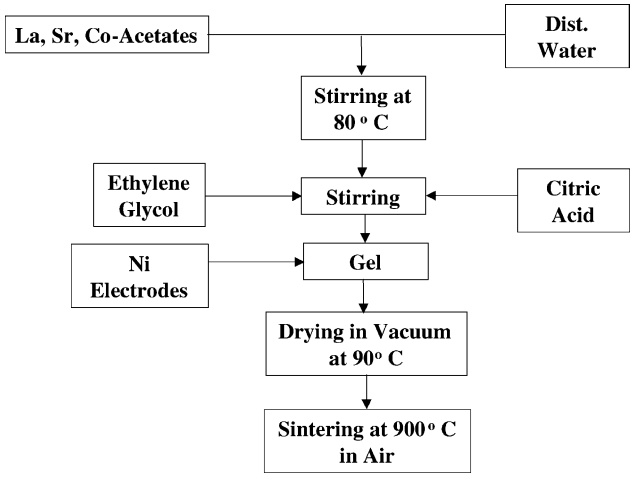

Fig. 2. Flow chart for the preparation of $La_{0.8}Sr_{0.2}CoO_3$ coated NiO by a sol–gel process.

2.4. Pot cell studies

In order to determine the solubility of nickel and LSC–NiO in molten carbonate, pot cell tests were carried out under cathode gas conditions. Pellet electrodes of 2.5 cm diameter were cut out from sintered nickel and LSC–NiO electrodes. They were weighed and carefully dropped inside an alumina crucible containing 100 g of molten carbonate $(Li_{0.62}K_{0.38})_2CO_3$ at 650 °C. Cathode gas (30% CO_2/70% air) was bubbled through the carbonate melt using alumina tubes. About 0.2 g of molten carbonate was taken from the melt approximately every 6 upto 200 h using an alumina rod. The molten carbonate sample was dissolved in 10% dilute acetic acid. Atomic absorption spectroscopy was used to analyze the concentration of dissolved nickel.

2.5. Electrochemical and material characterization

Half-cell performance studies were done in a 3 cm^2-lab cell used for our earlier studies [8]. Two identical LSC coated NiO cathodes were used as the working and counter electrodes. $(Li_{0.62}K_{0.38})_2CO_3$ eutectic embedded in a $LiAlO_2$ matrix was used as the electrolyte. Polarization studies were done using an oxidant gas composition of 70% air and 30% CO_2. The cathode gas flow rate consisted of N_2 60 cc/min, O_2 16 cc/min and CO_2 32 cc/min. Oxygen reference electrode (Au/67% CO_2/33% O_2) connected to the electrolyte tile with a salt bridge (50% $(Li_{0.62}K_{0.38})_2CO_3$ + 50% $LiAlO_2$) was used to monitor the polarization of cathode. The reference gas flow rate was kept at 10 cc/min. Electrochemical impedance spectroscopic studies were performed using a Model 1255 Schlumberger Frequency Analyzer. The electrode was stable during the experiments and its open circuit potential changed less than 1 mV. The impedance data generally covered a frequency range of 1 mHz to 100 kHz. A sinusoidal ac voltage signal varying by ±5 mV was applied in all cases. X-ray diffraction was used to confirm the formation of $La_{0.8}Sr_{0.2}CoO_3$ on the nickel electrodes and scanning electron microscope (SEM) was used to study the microstructure of the specimens.

3. Results and discussion

3.1. $La_{0.8}Sr_{0.2}CoO_3$ coating

The initial pH of the solution containing La, Sr and Co acetates was 5.38 and it reduced to pH 2.45 after citric acid and ethylene glycol addition. Due to this pH change, individual metal acetates precipitated. A clear solution was obtained when the pH of the solution was increased to 8.52 by adding ammonium hydroxide solution. Heating with a constant stirring for 24 h at 80 °C yielded a gel in which the sintered electrodes are dipped to get a $La_{0.8}Sr_{0.2}CoO_3$ precursor on the surface.

3.2. Scanning electron micrograph

Fig. 3 shows the SEM images of Ni and LSC coated nickel electrodes prepared by the above said procedure. The primary particle size according to Fig. 3 for nickel electrodes was in the range of 1.00–6.80 μm. Subsequent to LSC coating and sintering in air, the particles tend to agglomerate together. The LSC coated NiO had a good pore structure. However, detailed pore volume distribution analysis needs to be carried out to comment on the actual porosity and pore size distribution. The morphological difference between nickel and LSC coated nickel can be attributed to the LSC coating on nickel surface followed by sintering. No change is observed in the surface morphology of LSC coated NiO and LSC–NiO after immersion in molten carbonate for 200 h.

3.3. X-ray diffraction analysis

Figs. 4 and 5 show the XRD pattern obtained on the LSC coated samples. Fig. 4 shows the XRD patterns of $La_{0.8}Sr_{0.2}CoO_3$ powders obtained from the gel after heat treatment in different temperatures ranging between 300 and 900 °C. It is clearly seen that the compound formation starts only at 500 °C and crystalline product could be obtained at 900 °C. The $La_{0.8}Sr_{0.2}CoO_3$ formation onto the nickel electrodes was confirmed by matching the individual peaks. Fig. 5 shows the XRD pattern of LSC coated NiO sintered at 900 °C. Individual peaks correspond to $La_{0.8}Sr_{0.2}CoO_3$ and NiO are marked in the figure.

3.4. Stability tests

The short-term stability of LSC–NiO and bare nickel in molten carbonate eutectic were determined using pot tests. Atomic absorption spectroscopy (AAS) was used to analyze the dissolved nickel and cobalt in the melt. From AAS we

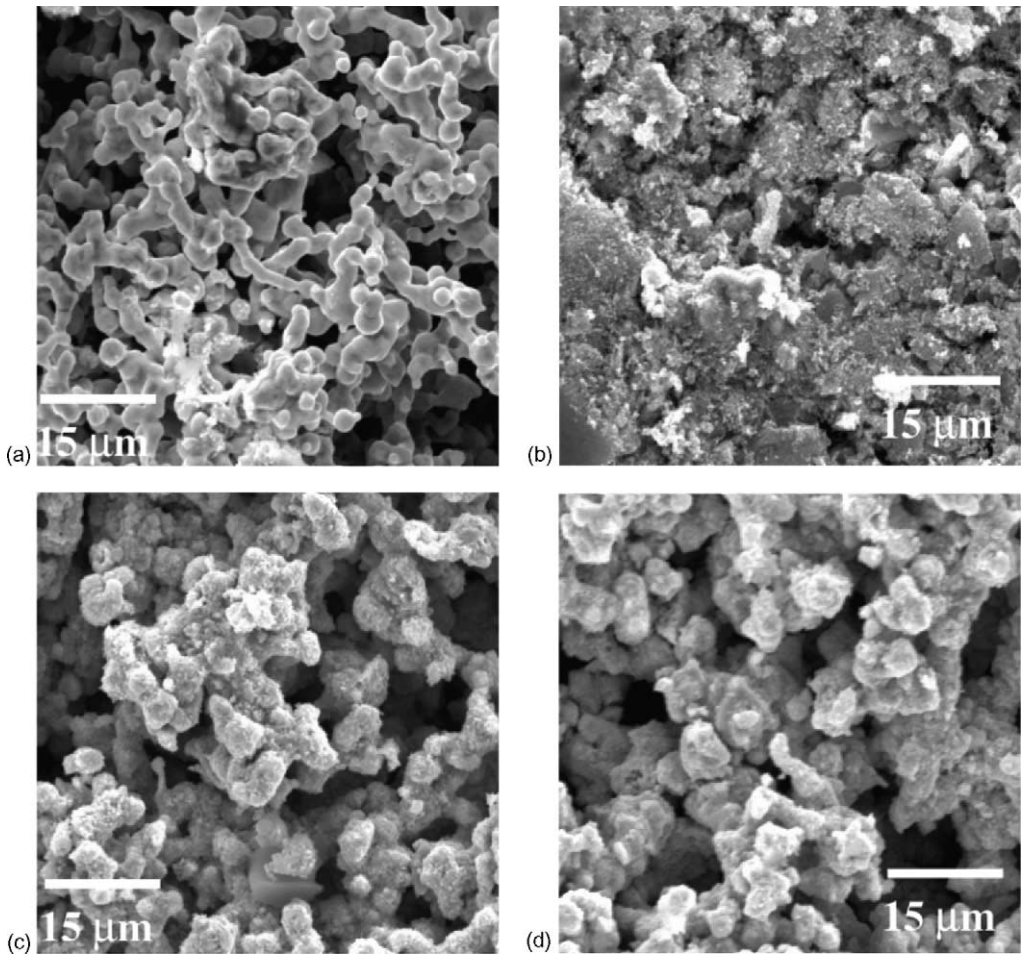

Fig. 3. SEM pictures of (a) sintered NiO, (b) $La_{0.8}Sr_{0.2}CoO_3$ precursor coated NiO electrode, (c) $La_{0.8}Sr_{0.2}CoO_3$ coated NiO electrodes, and (d) $La_{0.8}Sr_{0.2}CoO_3$ coated NiO electrodes after immersion in molten carbonate (magnification 2000×).

obtain the nickel ppm present in the solution of molten carbonate. Fig. 6 shows the results of AA analysis on the amount of dissolved nickel and cobalt in the carbonate melt as a function of time. As shown in the plot, the solubility of Ni^{2+} from bare nickel was higher when compared to that of LSC–NiO. The results indicate that LSC coating increases the stability of conventional NiO cathode molten carbonate environment. The amount of nickel increases with time and

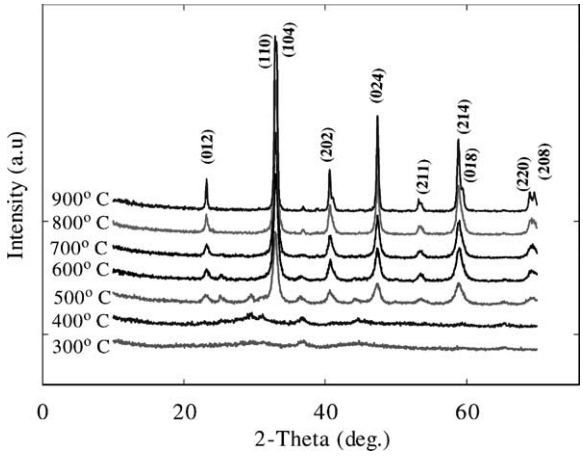

Fig. 4. X-ray diffraction patterns of $La_{0.8}Sr_{0.2}CoO_3$ obtained after different heat treatment of the gel precursor.

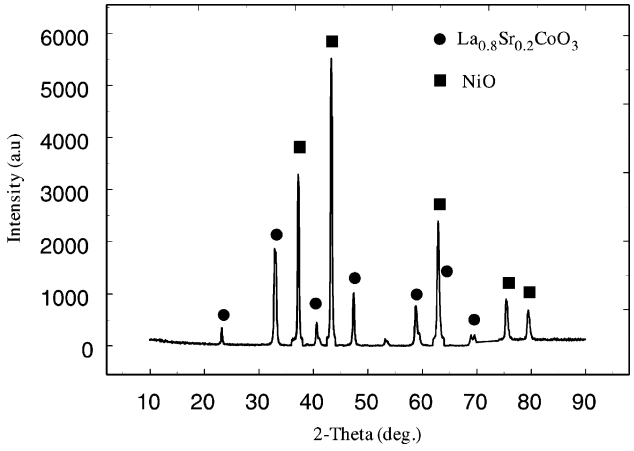

Fig. 5. X-ray diffraction patterns of $La_{0.8}Sr_{0.2}CoO_3$ coated NiO sintered at 900 °C.

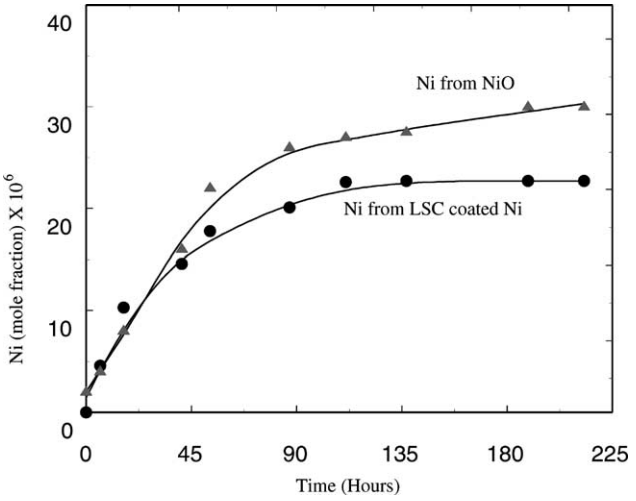

Fig. 6. Atomic absorption spectroscopy analysis of dissolved nickel in molten carbonate melt coming from $La_{0.8}Sr_{0.2}CoO_3$ electrodes during short-term stability tests.

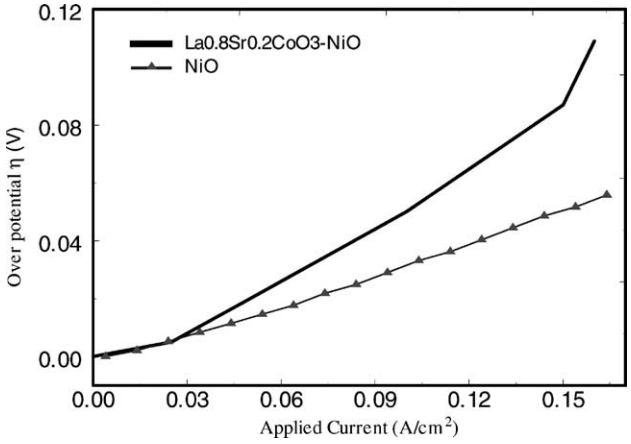

Fig. 7. Polarization behavior of $La_{0.8}Sr_{0.2}CoO_3$ coated NiO electrode and nickel electrode at 650 °C.

saturates after about 100 h. Similar results have been obtained in the literature for the solubility of Ni^{2+} ions in the carbonate melt [8–10]. Short-term stability test result shows that $La_{0.8}Sr_{0.2}CoO_3$ coating could prevent the nickel dissolution in the molten alkali carbonate melt.

3.5. Polarization studies

Polarization studies were carried out in a three electrode 3 cm^2-lab scale cell containing nickel/cobalt encapsulated nickel electrodes both as the working and counter electrodes and with gold (oxygen reduction) reference electrode. The electrodes were separated by a $LiAlO_2$ ceramic tile containing Li/K carbonate melt (62–38). The cells are connected to a gold/oxygen reference electrode through a salt bridge. The working electrode potential is monitored with respect to the reference electrode. The polarization characteristics of NiO and LSC–NiO cathodes were obtained by varying the current load. Fig. 7 compare the cathode polarization during the galvanodynamic scan for NiO and LSC–NiO cathode materials at cathode gas atmosphere. The current was scanned at 1 mA/s and the curves have been corrected for IR loss based on R_Ω calculated from impedance measurements. For NiO cathode shows a voltage loss of 55.9 mV and for LSC–NiO the voltage loss is of 109 mV. As can be seen from the polarization plot, the coated electrode suffers from mass transfer limitations. This suggest that the coating decreases the porosity for gas diffusion and electrolyte accommodation inside the electrode.

3.6. Electrochemical impedance spectroscopy (EIS) studies

In order to understand further the kinetics of oxygen reduction on LSC–NiO, impedance measurements were carried out at different gas compositions. EIS analysis was carried out at equilibrium potential (open circuit) on the NiO and LSC–NiO electrodes. Fig. 8 shows the impedance analysis of NiO electrode at different temperatures at a particular gas composition. The impedance response at any given temperature is characterized by the presence of high frequency loop and an extension at low frequencies. The high frequency plot has been associated with the charge transfer processes while the low frequency loop to a slow process (mass transfer or slow homogeneous reactions). The impedance response shown in Fig. 8 is similar in appearance to the ones obtained by Yuh and Selman [11,12] under similar conditions. As shown in Fig. 8, the cell temperature has a marked effect on the ac impedance. Increasing the temperature, a drastic decrease is observed in the charge transfer resistance, which is in agreement with the results obtained from polarization studies.

Fig. 9a–d shows the impedance response of LSC–NiO electrode as a function of different gas compositions at

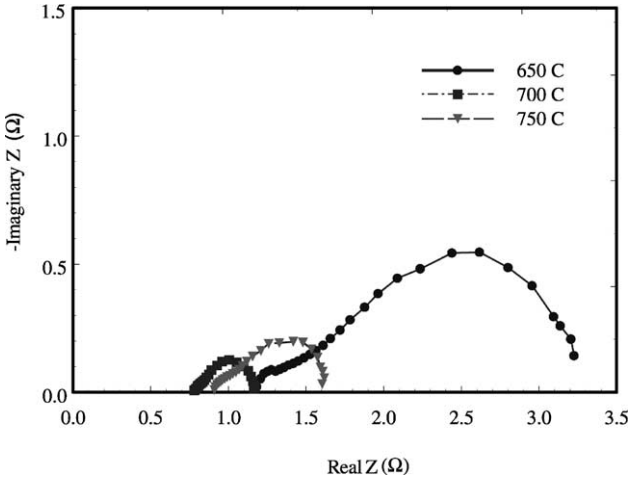

Fig. 8. Nyquist plots of NiO at different operating temperatures in standard cathode gas atmosphere (CO_2, 66%:O_2, 33%).

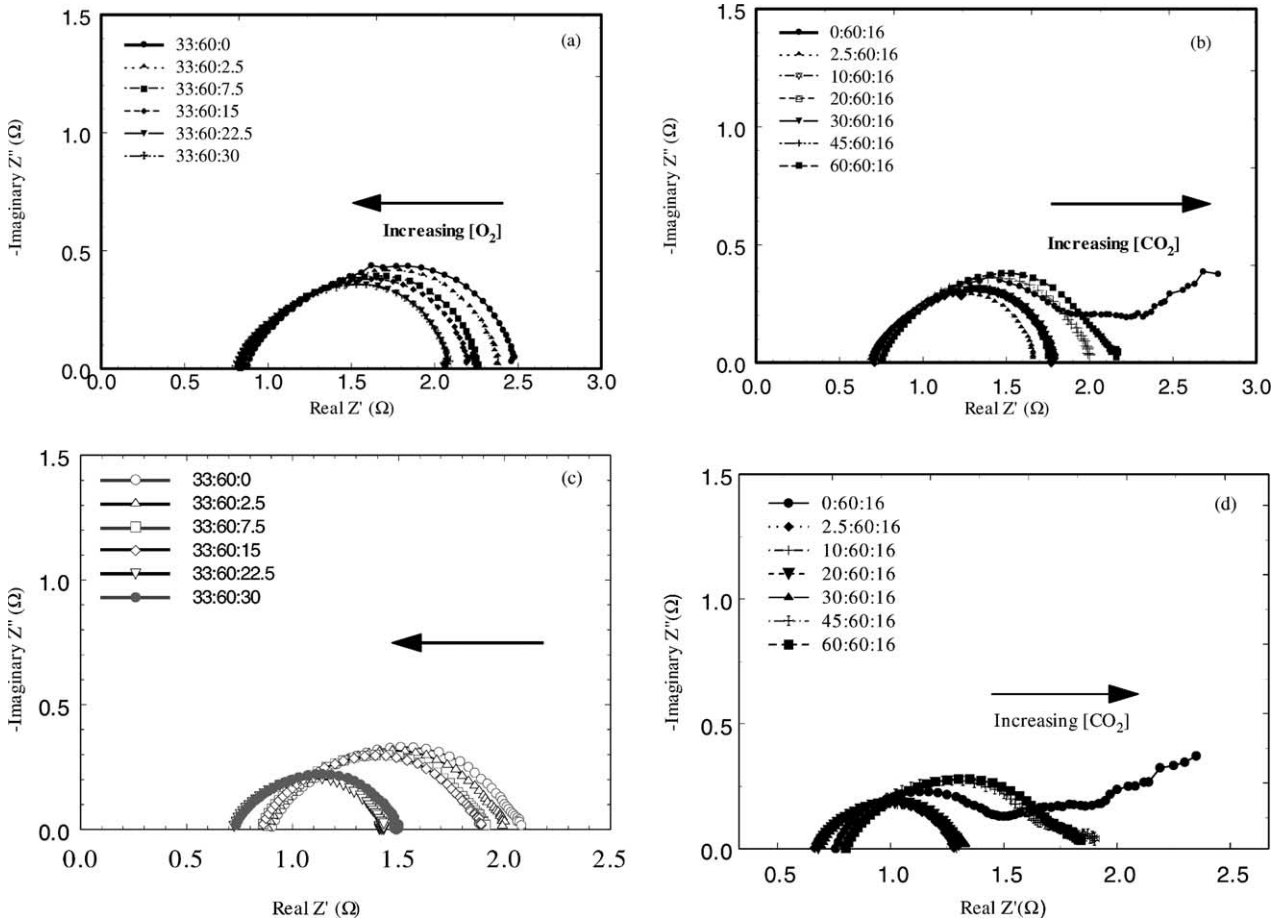

Fig. 9. Nyquist plots of impedance response of $La_{0.8}Sr_{0.2}CoO_3$ coated NiO electrode as a function of O_2 and CO_2 partial pressures at 650 °C (a and b), 700 °C (c and d).

different temperatures. The impedance responses appear differently in case of LSC–NiO when compared to those of NiO. The two distinct loopsoccurring at high and low frequencies in the case of NiO appear to be merged with each other in case of LSC–NiO. The effect of temperature clearly shows that the observed depressed semi circle loop includes both the charge transfer and mass transfer phenomenon. At higher temperature, the total impedance decreases suggesting that the observed effect could well be assumed as an increase in the diffusion coefficient and an increase in the kinetics for the oxygen reduction reaction. From Fig. 9a and b, it can also be seen that the effect of partial pressure of O_2 and CO_2 are antagonistic to each other. The magnitude of the impedance loop decreased on increasing the O_2 partial pressure. This clearly indicates a positive reaction order for oxygen and is similar to the response seen for NiO [12]. In case of CO_2, the impedance value increased with an increase in CO_2 partial pressures implying that the reaction order of CO_2 must be negative. A mass transfer limitation phenomenon was observed when no CO_2 was passed to the working electrode. The same effect was observed by Yuh and Selman with 2% CO_2 [13].

4. Conclusion

$La_{0.8}Sr_{0.2}CoO_3$ was coated on the state-of-the-art nickel electrode by a sol–gel method. LSC coating followed by sintering yielded electrodes with good pore structure. No significant difference in particle size of the LSC–NiO electrodes was seen before and after immersion in molten carbonate for 200 h. Short-term stability tests in molten carbonate melt at 650 °C showed that the coating is effective in reducing nickel dissolution. The impedance behavior of LSC–NiO in a half-cell is similar to that of conventional nickel oxide electrodes. Polarization studies showed 109 mV loss for an applied current of 160 mA/cm^2. However, extensive pore volume distribution studies need to be done to optimize the pore structure and porosity, which is expected to give minimum cathode polarization values.

References

[1] K. Tanimoto, Y. Miyazaki, M. Yanagida, S. Tanase, T. Kojima, N. Ohtori, H. Okuyama, T. Kodama, Denki Kagaku 59 (7) (1991) 619–622.

[2] K. Tanimoto, Y. Miyazaki, M. Yanagida, T. Kojima, N. Ohtori, T. Kodama, Denki Kagaku 63 (4) (1995) 316–318.
[3] L. Giorgi, M. Carewska, S. Scaccia, E. Simonetti, F. Zarzana, Denki Kagaku 64 (6) (1996) 482–485.
[4] M. Frank, J. Winnick, J. Appl. Electrochem. 19 (1989) 1–9.
[5] S.T. Kuk, Y.S. Song, K. Kim, J. Power Sources 83 (1999) 50–56.
[6] S.T. Kuk, Y.S. Song, S. Suh, J.Y. Kim, K. Kim, J. Mater. Chem. 11 (2001) 630–635.
[7] T. Fukui, S. Ohara, H. Okawa, T. Hotta, M. Naito, J. Power Sources 86 (2000) 340–346.
[8] A. Durairajan, H. Colon, B. Haran, R. White, B. Popov, J. Power Sources 104 (2) (2002) 157–168.
[9] K. Tanimoto, Y. Miyazaki, M. Yanagida, S. Tanase, T. Kojima, N. Ohtori, H. Okuyama, T. Kodama, Denki Kagaku 59 (7) (1991) 619.
[10] K. Ota, S. Mitsushima, S. Katao, S. Asano, H. Yoshitake, N. Kamiya, J. Electrochem. Soc. 139 (3) (1992) 667.
[11] C.Y. Yuh, J.R. Selman, J. Electrochem. Soc. 138 (12) (1991) 3642.
[12] C.Y. Yuh, J.R. Selman, J. Electrochem. Soc. 138 (12) (1991) 3649.
[13] C.Y. Yuh, J.R. Selman, AIChE J. 34 (12) (1998) 1949–1958.